JOURNAL OF SOLID STATE CHEMISTRY 114, 420–427 (1995)

Oxygen Coulometric Investigation of the Y–Cu–O System

R. A. Konetzki and R. Schmid-Fetzer

Technische Universität Clausthal, AG Elektronische Materialien, Robert-Koch-Strasse 42, D-38678 Clausthal-Zellerfeld, Germany

Received January 25, 1994; accepted May 24, 1994

Oxygen pressure and oxygen composition of phase equilibria involving the $Y_2Cu_2O_5$ and $YCuO_2$ phases in the Y_2O_3-Cu-CuO system have been studied by oxygen coulometric titration (OCT). The OCT-apparatus is specially designed to allow for a rapid quenching of the sample from a preselected equilibrium point. The phases present in the selected equilibrium are determined by X-ray diffraction. This simultaneous determination of oxygen pressure and composition and of the involved phases is considered to be superior to conventional e.m.f. studies in a complex oxide system where the equilibrium phases are questionable. It is shown that for a consistent and clear interpretation of the data that the combined use of stability diagrams and phase diagrams is essential and helpful. The decomposition conditions for $Y_2Cu_2O_5$ and $YCuO_2$ with decreasing temperature are discussed in detail. The $YCuO_2$ phase is identified as the "problem" phase, which is easily retained or even formed under metastable (supercooled) conditions. This metastable $YCuO_2$ disturbs the low temperature equilibria involving the $Y_2Cu_2O_5$ phase, thus leading to the large uncertainty observed for the decomposition temperature of $Y_2Cu_2O_5$.

1. INTRODUCTION

As part of an ongoing research project to provide basic thermodynamic and phase diagram information on high temperature superconductors, investigations in the Y–Cu–O ternary system have been carried out using an oxygen coulometric titration technique. The Y–Cu–O system is one of the faces of the Ba–Y–Cu–O quaternary system which contains the $Ba_2YCu_3O_{7-x}$ superconducting phase. Most of the investigations on the Ba–Y–Cu–O system have concentrated on the BaO–Y_2O_3–CuO pseudoternary, which is the section of the quaternary that is stable in air at higher temperatures (~1100 K). However, since $Ba_2YCu_3O_{7-x}$ has a range of oxygen stoichiometry that is sensitive to the oxygen partial pressure, it is important to study the ternary and quaternary systems at oxygen pressures both higher and lower than 0.21 bar.

The Y–Cu–O ternary, since Y_2O_3 is so much more stable than CuO, can be effectively represented as a Y_2O_3–CuO–Cu ternary subsystem below an oxygen pressure of 1 bar. In this subsystem there are six known phases: Y_2O_3, CuO, and $Y_2Cu_2O_5$, which are stable in air, and Cu metal, Cu_2O, and $YCuO_2$ (1), which are only stable at lower oxygen pressures. A $Y_2Cu_4O_5$ phase has also been reported and was found by (2) to exist in air between 1263 and 1378 K, but it is not known whether this phase is stable at lower temperatures and oxygen pressures.

The first thermodynamic measurements in the Y–Cu–O ternary were performed by (3), who determined the stability of $Y_2Cu_2O_5$ using an electromotive force (emf) technique on phase mixtures of $Y_2Cu_2O_5$–Y_2O_3–Cu_2O in the range 1173 to 1340 K. Two other emf studies have been performed on the same phase mixture, in the range 1173 to 1340 K (4) and in the range 1025 to 1220 K (5), and the results are similar to that of (3).

These results have been disputed by several studies (6–9) that claim that the equilibrium, $Y_2Cu_2O_5 + Y_2O_3 + Cu_2O$, does not exist due to the formation of a $YCuO_2$ phase at lower oxygen pressures. Wiesner *et al.* (7) performed thermogravimetric and oxygen coulometric titration (OCT) measurements on samples containing $Y_2Cu_2O_5$ and obtained $YCuO_2$ as the decomposition product in the temperature range 973 to 1223 K. Electromotive force (emf) measurements on phase mixtures containing $YCuO_2$ were performed in the ranges 873 to 1223 K (6), 1023 to 1273 K (8), and 1050 to 1330 K (9). Although all of these studies obtained roughly similar equilibrium oxygen pressures for the decomposition of $Y_2Cu_2O_5$ into $YCuO_2$, (6) and (9) obtained oxygen pressures that were orders of magnitude higher for the decomposition of $YCuO_2$ into Y_2O_3 + Cu than (7) and (8).

Suzuki *et al.* (10) performed an X-ray diffraction (XRD) study of samples in the Y_2O_3–CuO–Cu subsystem annealed at various temperatures in air or sealed under vacuum in silica ampoules. $YCuO_2$ was found to be stable at higher temperatures and lower oxygen pressure but decomposed into Y_2O_3 + Cu_2O at lower temperatures. Subsequent emf measurements of the phase mixture $Y_2Cu_2O_5$–Y_2O_3–Cu_2O at lower temperatures and $Y_2Cu_2O_5$–$YCuO_2$–Y_2O_3 and $Y_2Cu_2O_5$–$YCuO_2$–Cu_2O at higher temperatures support the XRD results. The $Y_2Cu_2O_5$–Y_2O_3–Cu_2O mixture was found to be slightly more stable than those containing $YCuO_2$ at temperatures lower

0022-4596/95 $6.00

than 1115 K. The oxygen pressure measurements for a $YCuO_2$–Y_2O_3–Cu phase mixture lie almost on the Cu_2O–Cu equilibrium line, indicating that $YCuO_2$ would be only slightly more stable than a mixture of Cu_2O + Y_2O_3.

The purpose of this work is to clarify these discrepancies using a specially designed OCT system. Oxygen can be titrated out of the closed system using a solid state electrolyte connected to a constant current or voltage source, while the oxygen pressure can be determined from the voltage across the titrating unit under open circuit conditions. The temperatures of the sample and titrating unit can be independently controlled while the sample can be quenched *in situ* without affecting the titrating unit and then quickly removed for XRD analysis. This allows the simultaneous determination of the decomposition pressure and products of a complex oxide without making any assumptions about the possible reaction products.

2. OCT APPARATUS

As stated in the introduction, the advantages of this OCT technique are that the sample and titrating unit temperatures are independently controlled and the sample can be quenched *in situ*. This is accomplished by using two independently controlled vertical tube furnaces, the lower of which can be lowered and swung away so that the sample may be water quenched without disturbing the titrating unit. A schematic diagram of the system is shown in Fig. 1 with the length dimension reduced as compared with the width.

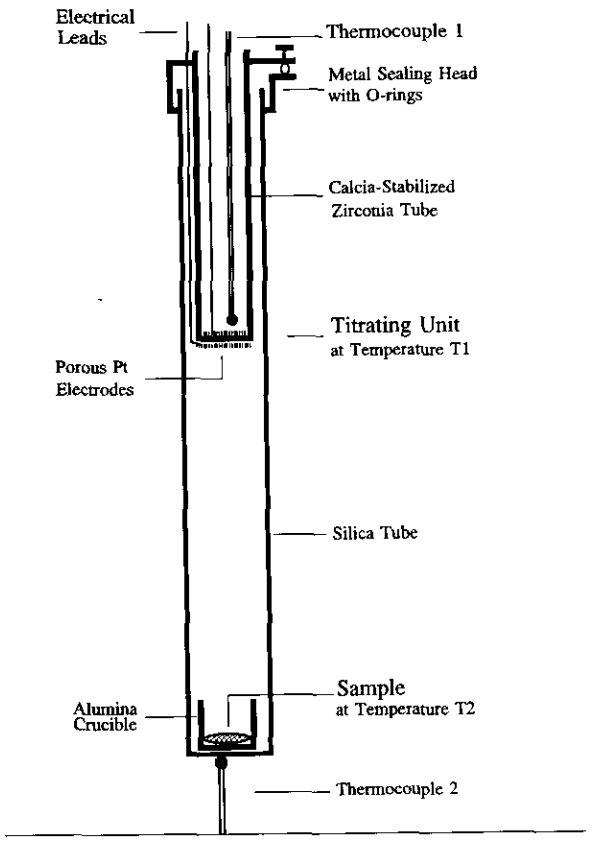

FIG. 1. Schematic view of the oxygen coulometric titration (OCT) apparatus.

The sample and titrating unit are contained in a long silica tube (500 mm long, 18 mm o.d., 12 mm i.d.) that is closed at the lower end where the sample is located. The titrating unit is constructed from a CaO-stabilized ZrO_2 tube (300 mm long, 10 mm o.d., 6 mm i.d.) that fits inside the silica tube. The whole system is sealed using a metal head that has O-ring seals to the silica and zirconia tubes and a valve to allow the system to be evacuated and backfilled. The system can hold a low vacuum, but is usually run at near atmospheric pressure to reduce the possibility of oxygen leakage into the system.

The preparation of the titrating unit is a multistep process. A 4 cm band of Ag paste was painted on the top portion of the zirconium tube and baked at 1073 K. This Ag band was lightly polished and serves two purposes: electrical contact for the sample lead and a better surface for the O-ring seal. The inside and outside of the closed end of the tube were painted with Pt paste and baked at 1273 K in order to produce porous electrodes. A sample lead made of Pt wire (0.3 mm diameter) was pasted to the outer electrode (facing the sample), baked at 1473 K, and then the other end of the lead was soldered to the Ag band. Later, another Pt wire is soldered to the Ag band on the air-exposed side of the O-ring seal in order to make electrical contact from the sample electrode to the current/voltage supply. Since the temperature of both solder joints are approximately the same, there is no net thermoelectric effect.

The electrical connection to the electrode inside the zirconia tube (reference electrode) is accomplished using an alumina rod with four channels: one for the reference lead wire (Pt), two for the thermocouple wires (PtRh18), and one to supply air to the reference electrode. The end of the reference lead wire was melted to form a sphere and is in a channel that is 2 mm longer than the others so that the thermocouple head does not touch the electrode and the air hole is not blocked. The reference lead wire was baked to the electrode at 1473 K and usually forms a bond that is stronger than the Pt wire itself. A small air pump connected to a filter, reservoir and throttle was used to provide a small, but constant flow of fresh air to the reference electrode through the fourth channel.

The samples were placed in small alumina crucibles that are lowered into the bottom of the silica tube. The sample temperature was measured using either of two thermocouples: PtRh18 at high temperatures or NiCr–Ni

for temperatures below 973 K. The exposed thermocouple heads are in physical contact with the bottom of the silica tube and thus separated from the sample by less than 10 mm.

3. EXPERIMENTAL PROCEDURE

The starting materials for the synthesis of the $Y_2Cu_2O_5$ were Y_2O_3 powder (99.99% pure) and CuO powder (99.999% pure). These were mixed in a 1 : 2 mole ratio, pressed into pellet form, and given a first annealing in air at 1173 K for 1 day. The pellets were then quenched, pulverized, and analyzed using XRD. This process was then repeated 4 or 5 times with annealing temperatures between 1173 and 1273 K and times of 3 to 4 days until no significant amounts of Y_2O_3 or CuO could be detected. The resulting XRD spectrum agrees well with that of $Y_2Cu_2O_5$, JCPDS card #33-511.

Two different master mixtures were made for use in the OCT experiments: $Y_2Cu_2O_5$ with 7 mass% Y_2O_3 or 7 mass% CuO. The required amount of Y_2O_3 or CuO was mixed with the pure $Y_2Cu_2O_5$ and annealed in air at 1173 K for 1 day in an alumina crucible. The Y_2O_3 or CuO was added so that a specific three-phase region would be entered when the $YCuO_2$ phase forms (referred to as Y- or Cu-rich samples). The master mixtures are known to be stable in air at the starting temperatures for titration: 1173 K for the high temperature experiments and 1023 K for the low temperature experiments.

For an individual OCT experiment approximately 10 mg of a master mixture in an alumina crucible was placed in the bottom of the silica tube, which was then fitted with the metal head and titrating unit. The furnaces were heated at approximately 0.1 to 0.2 K/s to the setpoints: 1023 K for the titrating unit and either 1023 or 1173 K for the sample. For constant current experiments the system valve was usually closed when the furnaces were near 500 K in order to build up the necessary overpressure to compensate for the later removal of the oxygen. In constant voltage experiments the system was left open to the air until the temperature set point was reached, was allowed to equilibrate for a few hours, and was then evacuated and backfilled with argon. Subsequently the constant voltage was applied. The reason for the different procedures is that in constant current experiments a detailed account of charge removed (amount of oxygen) is recorded in order to gain information on the stoichiometry of the phases. Since this is not possible in the constant voltage experiments in this study, a large amount of time and effort can be spared by starting with an argon-rich atmosphere.

Constant current experiments were performed first in order to determine the oxygen pressure in the first equilibrium with three condensed phases encountered at the starting temperature. Oxygen was removed step-wise from the system until the oxygen pressure remained constant. A waiting period of several hours to a day was required after each titration step to allow the system to reach equilibrium. The oxygen pressure was calculated using

$$p_{O_2} = 0.21\, p_{air} \exp[-4FE/RT], \qquad [1]$$

where E is the open circuit voltage across the titration unit measured using a high-impedance digital electrometer (± 0.1 mV), p_{air} is the atmospheric pressure in bar measured using a precision barometer, 0.21 is the assumed mole fraction of oxygen in the atmosphere, R is the gas constant, and F is the Faraday constant. A value of 11.605 K/mV was used for F/R. After the equilibrium pressure was fully established, the temperature was changed in 25-K steps in order to determine the temperature-dependence of the equilibrium pressure. The sample can then be quenched in order to determine the phases involved in the equilibrium or oxygen can be further titrated from the system until the next three-phase equilibrium is reached. From the amount of oxygen titrated out of the system during the decomposition, information about the phase stoichiometry can be obtained. In later experiments investigating the lower oxygen pressure equilibria, a constant voltage source was used because the extraction currents were below the capabilities of the constant current source (less than 100 μA).

4. EXPERIMENTAL RESULTS

In the preliminary experiments the three-phase equilibria were reached using the constant current method; then, the oxygen pressure was measured across the whole range of temperatures. However, it was observed that different results were obtained when the sample was started from 1023 K and the temperature was increased than when the temperature was decreased from 1173 K. The intersection of the two different sets of data occurred approximately near the transformation temperature, 1115 K, determined by (10) and it was observed that the oxygen pressure would eventually approach the higher oxygen pressure value (the thermodynamically more stable value in this case) if allowed to sit for several days. Thus the later experiments were confined to the temperature region either above 1123 K (high temperature) or below 1098 K (low temperature).

The results for the decomposition of $Y_2Cu_2O_5$ obtained for both the Y- and Cu-rich samples at high and low temperatures from constant current experiments are shown in Fig. 2 along with data from the literature. The high temperature results from Y- and Cu-rich samples are

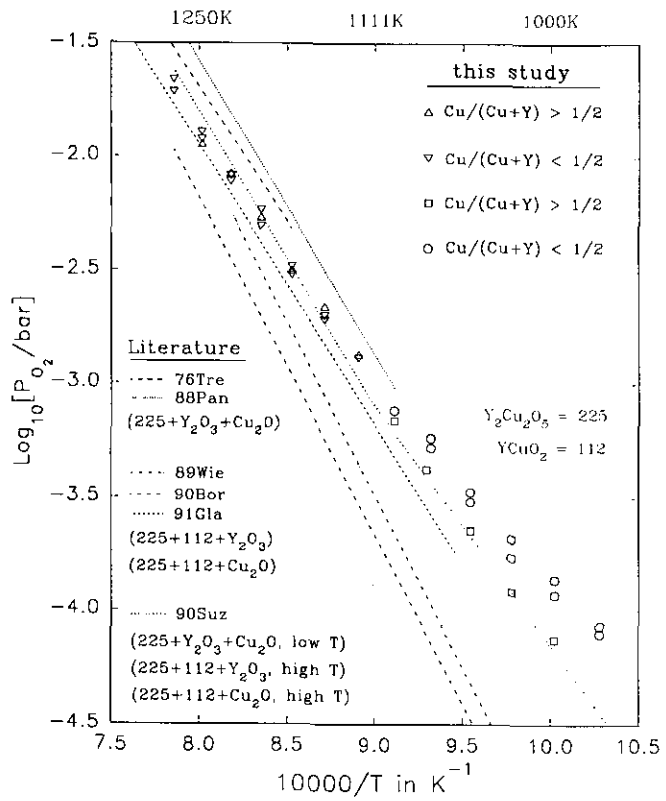

FIG. 2. Experimentally determined oxygen pressure from this OCT study compared to literature data, using mostly the emf method. References 76Tre, (3); 88Pan, (4); 89Wie, (7); 90Bor, (8); 91Gla, (9); 90Suz, (10).

almost identical and a linear regression of both sets of results are given by

$$\mathrm{Log}_{10}[p_{O_2}/\mathrm{bar}] = 7.144 - 11\,286/T \quad (T > 1106\ \mathrm{K}). \quad [2]$$

These data are consistent with the results from (10). The three-phase equilibria corresponding to Eq. [2] were identified by XRD analysis as $Y_2Cu_2O_5 + YCuO_2 + Y_2O_3$ for the Y-rich and $Y_2Cu_2O_5 + YCuO_2 + Cu_2O$ for the Cu-rich samples. The XRD spectrum for the $YCuO_2$ phase was identified as either the 6H-polytype or a mixture of the 2H and 3R polytypes of the delafossite type structure (1) since peaks characteristic to both types were found. The lattice parameters calculated for a 6H polytype from our spectra are: $a = 0.3521(2)$ nm, $b = 0.3521(1)$ nm, and $c = 3.4254(54)$ nm, where the number in parentheses is the error in the last digit.

In the low temperature region the Y-rich data are given by

$$\mathrm{Log}_{10}[p_{O_2}/\mathrm{bar}] = 4.635 - 8\,510/T \quad (T < 1106\ \mathrm{K}). \quad [3]$$

The intersection of Eqs. [2] and [3] occurs at 1106 K. If one considers only the Y-rich high-temperature data instead of Eq. [2], the intersection with the low-temperature Y-rich data occurs at 1115 K, which is very close to the result of (10), 1116 K, even though the data have different slopes. However, four phases, $Y_2Cu_2O_5 + Y_2O_3 + Cu_2O + YCuO_2$, were detected in the sample using XRD which means that the sample was not in thermodynamic equilibrium. Only three condensed phases are allowed by the Gibb's phase rule at constant temperature.

The Cu-rich low-temperature results are different from the Y-rich, but consistent with those from [10]. However, the Cu-rich low-temperature data intersect the high temperature results at a much lower temperature, 996 K, and XRD analysis of the sample also showed four phases: $Y_2Cu_2O_5 + YCuO_2 + Cu_2O + Y_2O_3$. Since the Cu-rich low-temperature results are almost collinear with the high temperature data, they may actually be a metastable extension of the $Y_2Cu_2O_5 + YCuO_2 + Cu_2O$ equilibrium. At low temperatures, $YCuO_2$ may form even though it may not be stable, if the oxygen pressure was reduced below the metastable extension of the $Y_2Cu_2O_5 + YCuO_2 + Cu_2O$ line. This metastable $YCuO_2$ was present as the nonequilibrium phase in both the Y- and Cu-rich four-phase mixtures at low temperature.

In order to study the $Y_2Cu_2O_5 + Y_2O_3 + Cu_2O$ equilibrium without the presence of the metastable $YCuO_2$, the constant voltage source was used with a Cu-rich sample. The voltage was first held constant at an oxygen potential a little below the CuO/Cu_2O equilibrium in order to reduce the CuO to Cu_2O, then slightly above the metastable $Y_2Cu_2O_5 + YCuO_2 + Cu_2O$ equilibrium in order to observe the $Y_2Cu_2O_5 + Y_2O_3 + Cu_2O$ equilibrium. Unfortunately, no equilibrium could be obtained. The voltage was then set at an oxygen potential below the metastable extension of the $Y_2Cu_2O_5 + YCuO_2 + Cu_2O$ equilibrium and oxygen was titrated out of the system for a day. When the voltage was turned off, the oxygen pressure rather rapidly increased and within several hours approached the previously obtained low-temperature Cu-rich results from the constant current experiments. However, if the sample was allowed to sit for several days, the oxygen pressure gradually increased and approached the results obtained for the Y-rich low-temperature sample. The same four phases were also observed in the XRD spectrum.

As was mentioned in the introduction, information on the stoichiometry of the phases can be obtained by keeping account of the amount of oxygen titrated out during the equilibrium. This was applied to several Y-rich high-temperature samples and it was found that the $Y_2Cu_2O_5 + Y_2O_3 + YCuO_2$ equilibrium was exited much earlier than expected from the known mass of the sample, indicating that $YCuO_2$ or $Y_2Cu_2O_5$ might be highly unstoichiometric. However, subsequent XRD analysis showed that the sample still contained $Y_2Cu_2O_5 + Y_2O_3 + YCuO_2$,

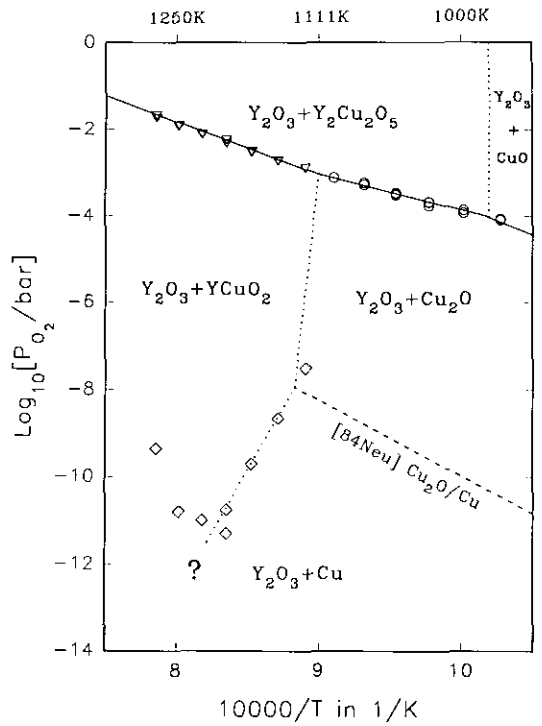

FIG. 3. Y-rich stability diagram, Cu/(Cu + Y) < ½, with experimental data from this study. The dashed line for Cu_2O/Cu is from Ref. 84Neu, (11).

demonstrating the incomplete decomposition of $Y_2Cu_2O_5$. This is another indication that the initial decrease in the oxygen pressure while titrating out in constant current mode was probably a change in kinetics due to oxygen having to diffuse through the decomposition products. Thus the sample must be allowed to equilibrate longer after each titration step. With 5 to 10 titration steps each lasting several days, 2 to 4 weeks would be required for a single sample at one temperature. Due to time considerations, this approach was discontinued.

In the final experiments the $YCuO_2 + Y_2O_3 + Cu$ equilibrium was investigated at high temperatures using a Y-rich sample. The voltage was set at an oxygen potential much lower than the $Y_2Cu_2O_5 + Y_2O_3 + YCuO_2$ equilibrium in order to decompose the $Y_2Cu_2O_5$, but not lower than the known Cu_2O/Cu equilibrium to be sure that the $YCuO_2$ would not start to decompose. After several days of titrating the extraction current became very low (1 nA) and the constant voltage was increased in order to find the $YCuO_2 + Y_2O_3 + Cu$ equilibrium. The equilibrium—confirmed by XRD results—was eventually found at very low pressures, closer to the results of (7, 8) than (6, 10, 9). However, these results, which are plotted in the Y–Cu–O partial stability diagram in Fig. 3, do not follow a straight line and are somewhat inconclusive.

5. DISCUSSION

5.1. Combining Stability and Phase Diagrams

The complex results obtained from this study of Y–Cu–O are difficult to understand in terms of the conventional simple "log p_{O_2} versus $1/T$" representation given in Fig. 2. In order to arrive at a consistent interpretation, it is essential to plot our experimental data in separate stability diagrams for the Y- and Cu-rich samples (Figs. 3 and 4), where the proper two-phase fields are denoted, separated by the partially measured three-phase lines. In addition, our data measured for the CuO/Cu_2O equilibrium occurring in the Cu-rich samples are given in Fig. 4 and in Fig. 3 for the Y-rich $YCuO_2 + Y_2O_3 +$ Cu equilibrium described in the previous paragraph. The Cu_2O/Cu equilibrium is taken from (11) and shown as a dashed line. The dotted lines are less well established three-phase equilibria. Both stability diagrams have to be checked for consistency with isothermal sections of the ternary phase diagram, given for three selected temperatures in Fig. 5.

For example, if we follow the titration run of a Y-rich sample at 1073 K in a comparison of Figs. 3 and 5b, the starting point may be at 10^{-1} bar oxygen pressure in the two-phase field $Y_2O_3 + Y_2Cu_2O_5$. Upon titrating oxygen out of the sample, the three-phase line $Y_2O_3 + Y_2Cu_2$

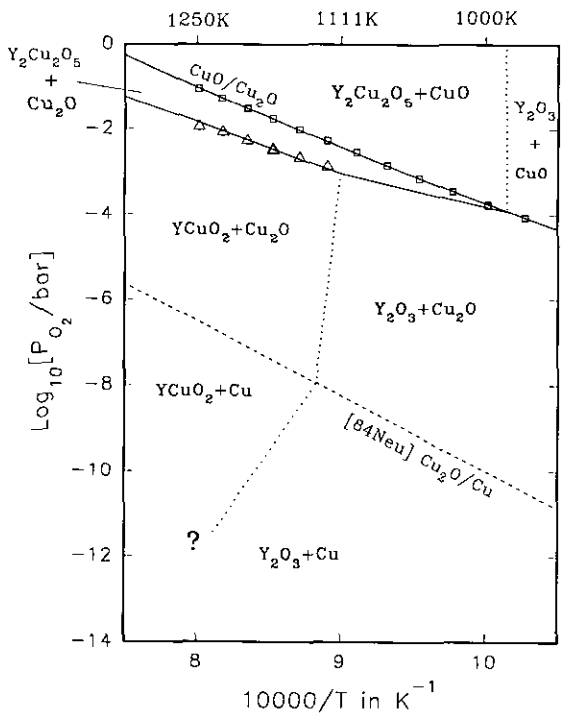

FIG. 4. Cu-rich stability diagram, Cu/(Cu + Y) > ½, with experimental data from this study. The dashed line for Cu_2O/Cu is from Ref. 84Neu, (11).

O_5 + Cu_2O is encountered at $10^{-3.3}$ bar in Fig. 3 and the decomposition of $Y_2Cu_2O_5$ begins. The same three-phase field is entered in Fig. 5b by reducing the oxygen content of the sample at the constant Y/Cu ratio. Further decrease in oxygen content is accomplished by reducing the amount of $Y_2Cu_2O_5$ at constant oxygen pressure until the two-phase field Y_2O_3 + Cu_2O is entered (given as a single tie line in Fig. 5b in view of the small solid solubilities). The oxygen pressure in this two-phase field is lowered with further out-titration and the three-phase line Y_2O_3 + Cu_2O + Cu in Fig. 3 is encountered at $10^{-9.3}$ bar, corresponding to the three-phase triangle in Fig. 5b. Finally, the two-phase equilibrium Y_2O_3 + Cu will be entered.

Following the same titration run for a Cu-rich sample, it is evident from Figs. 4 and 5b that one additional three-phase equilibrium must be passed (CuO + Cu_2O + $Y_2Cu_2O_5$) and also that above $10^{-3.3}$ bar the phases in equilibrium ($Y_2Cu_2O_5$ + Cu_2O) are different compared to the Y-rich sample (Y_2O_3 + $Y_2Cu_2O_5$). Similar considerations are valid for the other temperatures. This clearly demonstrates the superiority of interpreting the data in the complementary Figs. 3 to 5 compared to the conventional representation in Fig. 2.

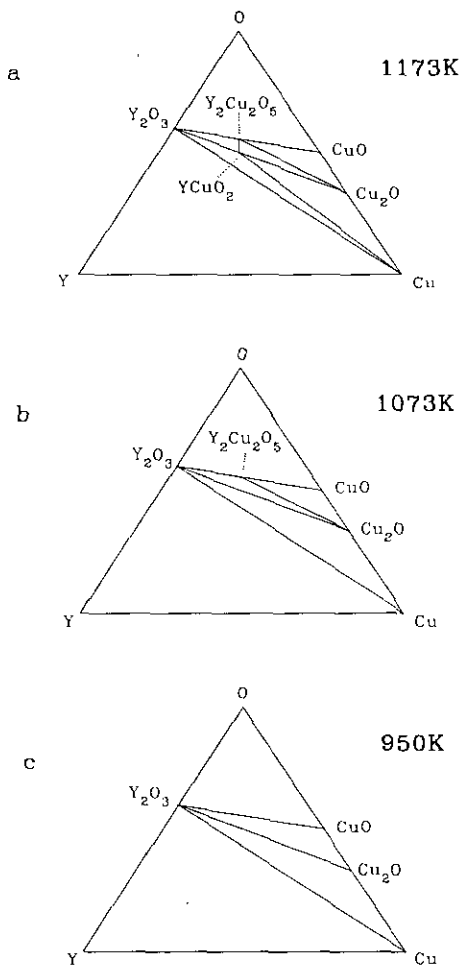

FIG. 5. Isothermal sections of the Y_2O_3–Cu–CuO subsystem in the ternary Y–Cu–O phase diagram at (a) 1173, (b) 1073, and (c) 950 K. The decomposition temperature of $Y_2Cu_2O_5$ is uncertain. Triangles are scaled in at.%.

It is interesting to note that our high-temperature p_{O_2} data measured along the equilibria $Y_2Cu_2O_5$ + $YCuO_2$ + Y_2O_3 (Fig. 3) and $Y_2Cu_2O_5$ + $YCuO_2$ + Cu_2O (Fig. 4) are virtually identical, given jointly by Eq. [2]. In the graphical presentation of Fig. 3 this line intersects the low temperature $Y_2Cu_2O_5$ + Y_2O_3 + Cu_2O data at 1106 K and $10^{-3.06}$ bar. This four-phase point $Y_2Cu_2O_5$ + $YCuO_2$ + Y_2O_3 + Cu_2O is exactly the same as the one in Fig. 4 although the phase combinations in some of the adjoining two-phase fields are different. The same remark applies to the four-phase point $YCuO_2$ + Y_2O_3 + Cu_2O + Cu at about 10^{-8} bar in Figs. 3 and 4. Both four-phase points are end points of the three-phase line $YCuO_2$ + Y_2O_3 + Cu_2O, representing the decomposition limit of the $YCuO_2$ phase with decreasing temperature.

5.2. *Decomposition of $YCuO_2$*

This three-phase line $YCuO_2$ + Y_2O_3 + Cu_2O, shown as the dotted line in Figs. 3 and 4, is given with a slight temperature variation to indicate the possibility of a range of oxygen stoichiometry in $YCuO_2$. This line would be vertical for an exactly stoichiometric $YCuO_2$ phase. In that case the decomposition of $YCuO_2$ would be degenerate into the reaction $YCuO_2 \rightleftarrows (\frac{1}{2})Y_2O_3 + (\frac{1}{2})Cu_2O$ (seemingly equilibrated with both $Y_2Cu_2O_5$ and Cu in an isothermal section of the phase diagram at 1106 K).

This seemingly five-phase equilibrium splits properly into the following two four-phase equilibria in the phase diagram if an oxygen excess solubility range is considered: a eutectoid reaction,

$$YCuO_{2+x} \rightleftarrows xY_2Cu_2O_5 + (\tfrac{1}{2} - x)Y_2O_3 + (\tfrac{1}{2} - x)Cu_2O \quad \text{(at } 10^{-3.06} \text{ bar and 1106 K)};$$

and a transition type reaction,

$$YCuO_{2+x} + 2xCu \rightleftarrows (\tfrac{1}{2})Y_2O_3 + (\tfrac{1}{2} + x)Cu_2O \quad \text{(at } \approx 10^{-8} \text{ bar and } \gtrapprox 1106 \text{ K)}.$$

In case of a small oxygen deficiency (negative value for the solubility x), these two reactions have to be inverted accordingly. It should be pointed out that quantitative data for a solubility range are lacking. The $YCuO_2$ phase will be considered as stoichiometric for the following calculation of the Gibbs energy of formation.

Our experimental p_{O_2} data given in Eqs. [2] and [3] correspond to the following two reactions:

$$Y_2Cu_2O_5 \rightleftarrows 2\ YCuO_2 + \tfrac{1}{2}\ O_2, \quad [4]$$

and

$$Y_2O_3 + Cu_2O + \tfrac{1}{2}\ O_2 \rightleftarrows Y_2Cu_2O_5. \quad [5]$$

The formation of $YCuO_2$ from the oxides is obtained by addition:

$$Y_2O_3 + Cu_2O \rightleftarrows 2\ YCuO_2. \quad [6]$$

It should be noted that the value of p_{O_2} in reaction [4] is fixed because it was found to be practically the same in the two adjoining three-phase equilibria $Y_2Cu_2O_5 + YCuO_2 + Y_2O_3$ and $Y_2Cu_2O_5 + YCuO_2 + Cu_2O$. The corresponding standard Gibbs energies of formation are given by

$$\Delta G^\circ_{\{4\}} = (108\,032 - 68.384\ T)\ \text{J/mol} \quad [4a]$$

$$\Delta G^\circ_{\{5\}} = (-81\,459 + 44.367\ T)\ \text{J/mol} \quad [5a]$$

$$\Delta G^\circ_{\{6\}} = (+26\,573 - 24.017\ T)\ \text{J/mol}. \quad [6a]$$

The driving force for the decomposition of $YCuO_2$ calculated from Eq. [6a] is small, only 1.3 kJ per mol of $YCuO_2$ at 1000 K, corresponding to a supercooling of 106 K. This value represents an upper limit since it results from the different slopes of the log p_{O_2} data, which were almost the same for the Cu-rich samples.

This low driving force and a possibly high activation barrier for the decomposition of $YCuO_2$ is assumed to be responsible for the difficulty in obtaining the $Y_2Cu_2O_5 + Y_2O_3 + Cu_2O$ equilibrium without the presence of (metastable) $YCuO_2$, found in all the low-temperature samples. The problem with metastable $YCuO_2$ is compounded since its formation occurs very easily. The $YCuO_2$ phase was even found in the sample starting with $Y_2Cu_2O_5 + CuO$ at fixed temperatures well below 1106 K by just reducing p_{O_2} in various ways. This $YCuO_2$ must have been formed within the $Y_2O_3 + Cu_2O$ field of Fig. 4, once p_{O_2} drops below the metastable extension of the $Y_2Cu_2O_5 + YCuO_2 + Cu_2O$ equilibrium line.

5.3. *Decomposition of $Y_2Cu_2O_5$*

The intersection of the $Y_2Cu_2O_5 + Y_2O_3 + Cu_2O$ line with the CuO/Cu_2O equilibrium defines the decomposition temperature of $Y_2Cu_2O_5$, shown as the dotted line in both Figs. 3 and 4. This temperature, 970 K, is uncertain because of the uncertainty in the $Y_2Cu_2O_5 + Y_2O_3 + Cu_2O$ equilibrium line. No data points are shown for this line in Fig. 4, which is taken to be the same as in Fig. 3, since both lines should describe the same equilibrium. The actual measured data points from the Cu-rich samples in Fig. 4 are not shown; they almost follow the metastable extension of the $Y_2Cu_2O_5 + YCuO_2 + Cu_2O$ line from higher temperatures, similar to the data of (10). These data, given in Fig. 2, would intersect the CuO/Cu_2O equilibrium at ≈840 K, thus setting a lower limit for the decomposition temperature of $Y_2Cu_2O_5$.

This uncertainty is also reflected by the range of decomposition temperatures calculated for the reaction $Y_2Cu_2O_5 \rightleftarrows Y_2O_3 + 2CuO$ from the literature data of ΔG°: 916 K (10), 913 K (4), 908 K (3), 744 K (6) and 650 K (5). An unreasonably high value of 5463 K may be calculated from the ΔG° data of (7) which is not considered further because of the inverted temperature dependence (negative entropy of formation).

The basic reason for this uncertainty is the occurrence of the nonequilibrium $YCuO_2$ phase as the fourth phase in the samples below 1106 K. Considering the persistence of this metastable $YCuO_2$ in all our different approaches to a true equilibrium, it may be assumed that $YCuO_2$ was also present in the corresponding studies reported in the literature. One progress due to the present OCT technique with XRD analysis of quenched samples is that we have conclusively identified $YCuO_2$ to be the "problem" phase.

6. CONCLUSION

- The OCT technique with *in situ* quenching and subsequent XRD phase analysis is considered to be superior to conventional emf studies in an oxide system where the equilibrium phases are questionable.
- The combination of stability diagrams and isothermal sections of the phase diagram is essential for a consistent and conclusive interpretation of the experimental data. Confusion may arise in a simple conventional "log p_{O_2} versus $1/T$" presentation of all the data without noting the different adjoining phase fields and their interrelation with the phase diagram.
- The decomposition of the $YCuO_2$ phase with decreasing temperature according to the reaction $YCuO_2 \rightleftarrows (\tfrac{1}{2})Y_2O_3 + (\tfrac{1}{2})Cu_2O$ occurs at 1106 K or probably at a higher temperature in the range 1115 to 1106 K. This decomposition is very sluggish. On the other hand, the formation of $YCuO_2$ occurs easily, even under metastable conditions.
- The decomposition of the $Y_2Cu_2O_5$ phase with decreasing temperature according to the reaction $Y_2Cu_2O_5 \rightleftarrows Y_2O_3 + 2CuO$ is much more uncertain. It may occur at 970 K or probably at a lower temperature in the range 970 to 840 K. The reason for this uncertainty is that metastable $YCuO_2$ is present at lower temperatures in the $Y_2Cu_2O_5 + Y_2O_3 + Cu_2O$ equilibrium.

ACKNOWLEDGMENT

Financial support by the SUPERDATA project of Brite-Euram, contract No. BREU-0203-C, is gratefully acknowledged.

REFERENCES

1. T. Ishiguro, N. Ishizawa, N. Mizutani, and M. Kato, *J. Solid State Chem.* **49,** 232 (1983).
2. A. M. Gadalla and P. Kongkachuichay, *J. Mater. Res.* **6,** 450 (1991).
3. Yu. D. Tretyakov, A. R. Kaul, and N. V. Makukhin, *J. Solid State Chem.* **17,** 183 (1976).
4. R. Pankajavalli and O. M. Sreedharan, *J. Mater. Sci. Lett.* **7,** 714 (1988).
5. R. Shimpo and Y. Nakamura, *J. Jpn. Inst. Metals Sendai* **54,** 549 (1990).
6. G. M. Kale and K. T. Jacob, *Chem. Mater.* **1,** 515 (1989).
7. U. Wiesner, G. Krabbes, and M. Ritschel, *Mater. Res. Bull* **24,** 1261 (1989).
8. K. Borowiec and K. Kolbrecka, *J. Less-Common Met.* **163,** 143 (1990).
9. F. Glathe, H. Oppermann, and W. Reichelt, *Z. Anorg. Allg. Chem.* **606,** 41 (1990).
10. R. O. Suzuki, S. Okada, T. Oishi, and K. Ono, *Mater. Trans. JIM* **31,** 1078 (1990).
11. J. P. Neumann, T. Zhong and Y. A. Chang, *Bull. Alloy Phase Diagrams* **5,** 136–140 (1984).